Geochemical Perspectives Letters

Geobarometric evidence for a LM/TZ origin $CaSiO_3$ in a sublithospheric diamond

P.-T. Genzel, M.G. Pamato, D. Novella, L. Santello, S. Lorenzon, S.B. Shirey, D.G. Pearson, F. Nestola, F.E. Brenker

Supplementary Information

The Supplementary Information includes:

- Material and Methods
- Figures S-1 to S-3
- Supplementary Information References

Material and Methods

Sample. The investigated diamond, Juina São Luiz 05192014 1a 055 (hereafter JU55; Fig. 1a, b), comes from the alluvial diamond deposit of the São Luiz River, in the Juina Area, Mato Grosso State, Brazil. JU55 is a 0.16 carat diamond with dimensions of approximately 4.5 × 3 × 1.5 mm^3. In this study, we performed a non-destructive analysis of a single phase breyite inclusion (named inclusion 2) with a maximum dimension of ~120 µm, which is still enclosed in its host diamond (Fig. 1a, black square in Fig. 1c) by single-crystal X-ray diffraction (hereafter SCXRD). Further inclusions of JU55 were analysed by micro-Raman spectroscopy (hereafter MRS) and optical microscopy.

In situ single-crystal X-ray diffraction. The X-ray data were collected using a Rigaku Oxford Diffraction SuperNova diffractometer equipped with a Mova X-ray micro-source and a Dectris Pilatus 200 K area detector at the Department of Geosciences of the University of Padova, Italy. For the measurements, a Mo$K\alpha$ micro-X-ray source operating at 50 kV and 0.8 mA with a radiation wavelength of 0.71073 Å was used. The detector-to-sample distance was set to 68 mm. The size of the beam spot is about 120 µm. Before the actual measurement, several scans at different phi-angles were performed to test the precise position of the inclusion under the X-ray beam. Data reduction was performed using the CrysAlis^{Pro} software (Rigaku Oxford Diffraction).

Micro-Raman spectroscopy. *In situ* MRS was performed at the Department of Geosciences of the University of Padova, Italy, using a WITec alpha300 R Raman Imaging Microscope equipped with a green laser (532 nm). The single spectra were collected using a 50× long working distance objective. The Raman system was set with 300 lines/mm grating. For every inclusion, two spectra were collected with two different frequency ranges. The first spectrum was collected over a frequency range extending from 0 to 4000 cm^{-1} and the second from 200 to 1250 cm^{-1}. Spectra collection over a shorter frequency range was performed to obtain higher intensities for the single inclusion Raman bands, as the intensity of the first order diamond band located at 1332 cm^{-1} is much higher than the intensity for the Raman bands of the various inclusions trapped inside the diamond. Each spectrum was accumulated 10 times using an

integration time of 10 s; at the end of the acquisition the spectra were merged. The Raman instrument was calibrated with a silicon plate for intensity and correct position of the 520 cm^{-1} silica band. Background correction, with a linear function and Lorentzian fitting were done using the open-source software Fityk (Wojdyr, 2010).

Optical microscopy. Optical microscopy was performed with a Keyence digital microscope VHX-6000 at the Geoscience Institute, Goethe University Frankfurt. Two objectives with magnifications from 20× to 200× and from 200× to 2000× were used to identify the mineral inclusions in JU55.

Breyite inclusions in groups 1 and 2. Beyond the inclusion 2 in Figure 1a within the black square, the same figure shows within the largest white rectangle two further groups of inclusions, which are here called group 1(1) and group 1(2). Single-crystal X-ray diffraction on these two groups of inclusions identified them as further breyites. The unit-cell parameters and volumes of these four breyite are:

Group 1
1(1a) a = 6.662(9) Å, b = 6.571(13) Å, c = 9.165(15) Å, α = 83.6(2)°, β = 69.8(1)°, γ = 77.1(2)°, V = 364.6(10) Å^3
1(1b) a = 6.631(10) Å, b = 6.627(11) Å, c = 9.185(16) Å, α = 84.2(2)°, β = 69.7(2)°, γ = 77.3(2)°, V = 369.1(9) Å^3

Group 2
1(2a) a = 6.641(14) Å, b = 6.651(9) Å, c = 9.267(17) Å, α = 69.9(1)°, β = 84.4(2)°, γ = 77.7(1)°, V = 375(1) Å^3
1(2b) a = 6.608(13) Å, b = 6.614(19) Å, c = 9.25(2) Å, α = 69.8(2)°, β = 83.8(2)°, γ = 76.7(2)°, V = 369(2) Å^3

The volumes of these four inclusions provided residual pressures P_{inc} much lower than that found for inclusion 2; in detail:

Inclusion 1(1a), P_{inc} = 2.982 GPa
Inclusion 1(1b), P_{inc} = 1.818 GPa
Inclusion 1(2a), P_{inc} = 0.394 GPa
Inclusion 1(2b), P_{inc} = 1.843 GPa

The simultaneous presence of inclusions of the same mineral showing different residual pressures is quite common in super-deep diamonds (Anzolini *et al.*, 2016). This is mainly due to the common fractures present in super-deep diamonds, which cause a pressure release. In these cases, the calculation of the pressure of formation is often useless as it will only represent a minimum pressure.

Inclusion phase identification by Raman spectroscopy. *In situ* micro-Raman analyses on inclusion 13 resulted to be magnesite (Fig. S-1), while for inclusion 9 they resulted to be the two coexisting TiO_2 polymorphs rutile and anatase (Fig. S-2). Micro-Raman spectroscopy was also useful to confirm the breyite identification carried out by X-ray diffraction for inclusions of groups 1 and 2 (see Fig. 1a within the white rectangle). In detail, we collected a few Raman spectra, which were compared with the Raman spectrum of breyite holotype in Brenker *et al*. (2021). In Figure S-3, we plotted two typical Raman spectra of breyite found for groups 1 and 2.

The concept of the isomeke. As well described in the extensive review by Angel *et al.* (2022), in the exact moment when a diamond entraps an inclusion, they are at the same pressure and temperature; under these conditions, the inclusion completely fills the void within the diamond, which means that the void inside the diamond and the inclusion must occupy the same volume. Once the entrapment is completed and the diamond moves, if "*the pressure and temperature change in such a way that the natural expansion and contraction of a free crystal of the inclusion exactly matches that of the host diamond, the inclusion will continue to exactly fit the void space in the diamond without*

the application of any additional stress" (Angel *et al.*, 2022). The pressure–temperature values lie on a line that is called "isomeke" (Rosenfeld and Chase, 1961; Adams *et al.*, 1975), which is defined by the difference in the thermoelastic properties (volume thermal expansion and compressibility) of diamond and its inclusion. Thus, if we have available an equation of state for the host-inclusion system, we can calculate an isomeke and this is what we have done in this work using the equation of state of breyite (Anzolini *et al.*, 2016) and that of diamond (Angel *et al.*, 2015). In Figure 2, we have plotted a coloured area which is constituted by a series of isomekes covering all *P*-*T* values within the experimental uncertainty from our unit-cell volume calculation (and thus from our P_{inc}).

Supplementary Figures

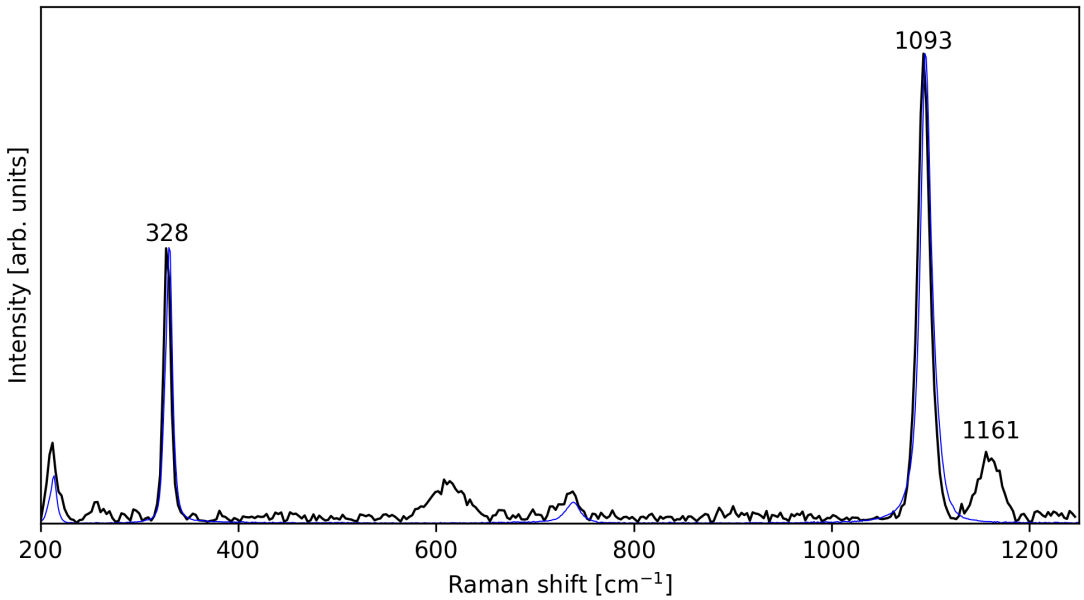

Figure S-1 Raman spectrum of magnesite (inclusion 13 in Fig. 1a) compared to the magnesite reference R040114 from the RRUFF Raman database (Lafuente *et al.*, 2016).

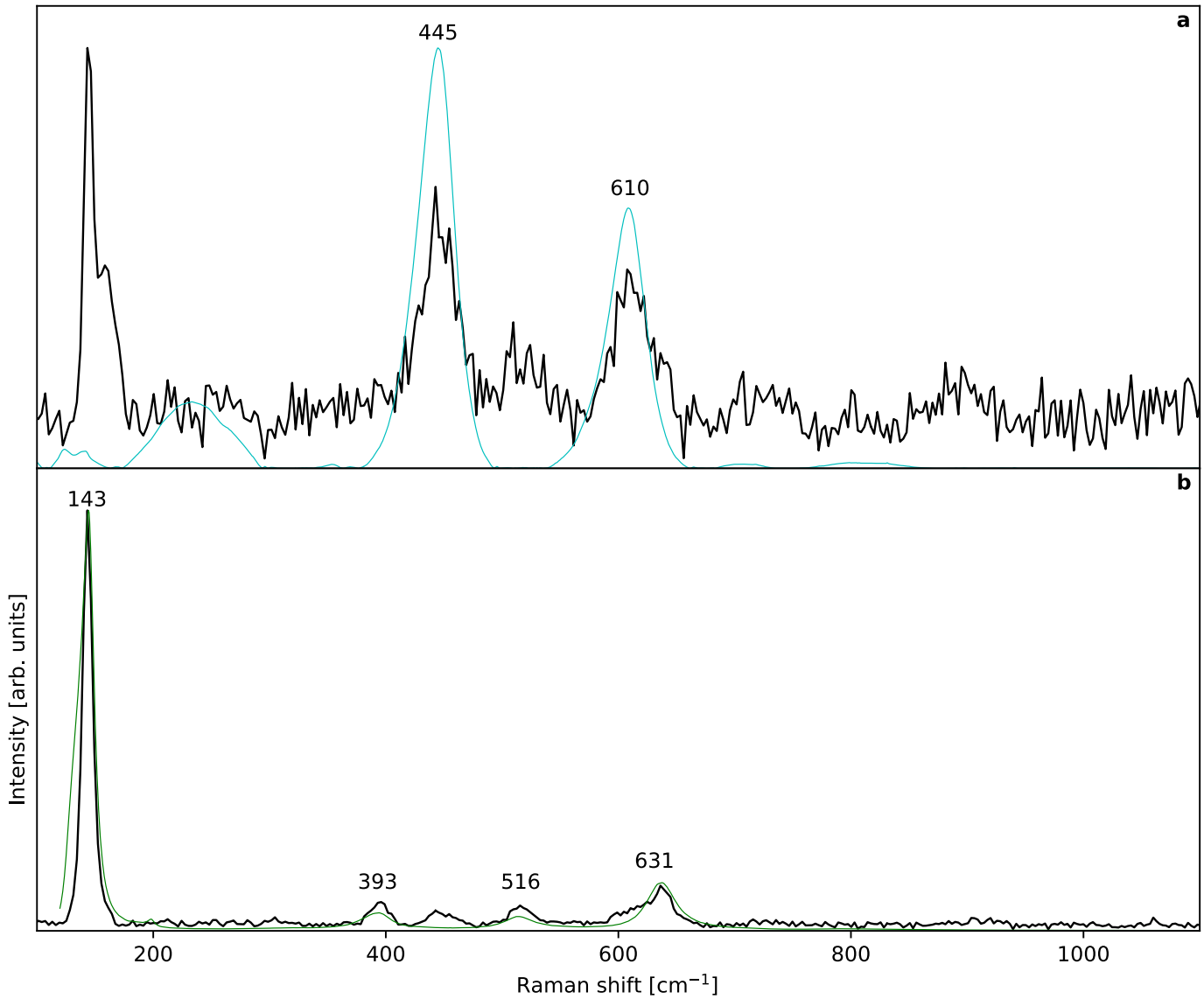

Figure S-2 Raman spectra of rutile and anatase (inclusion 9 in Fig. 1a) compared to the rutile reference R060493 and anatase reference R070582 from RRUFF Raman database (Lafuente *et al.*, 2016). Our data are plotted in black in both **(a)** and **(b)**.

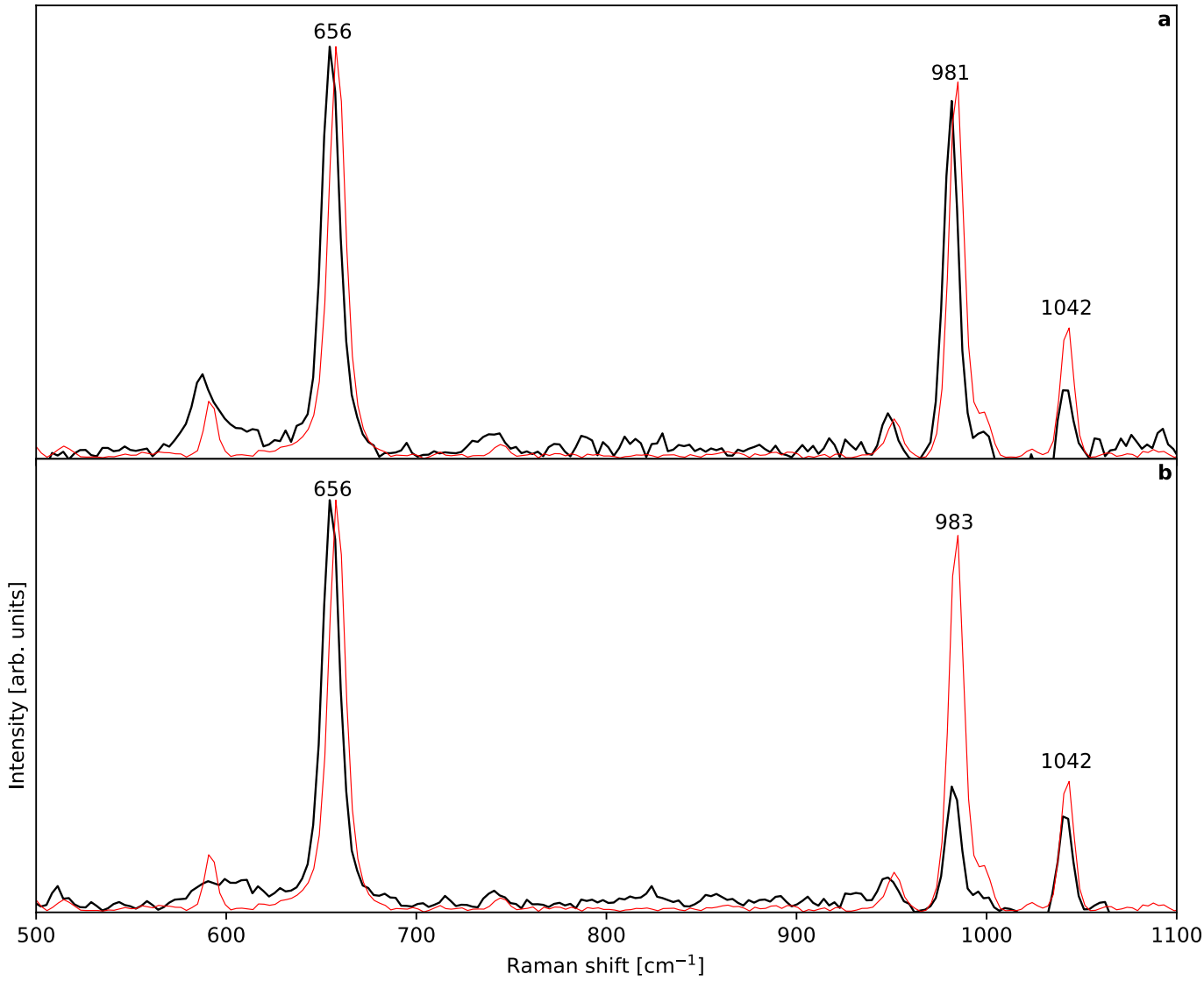

Figure S-3 Raman spectra of two breyites [inclusions from groups 1(1) and 1(2) in Fig. 1a] compared to the Raman spectrum of the holotype breyite by Brenker *et al*. (2021). In detail, in **(a)** we plotted a breyite from group 1(1) and in **(b)** a breyite from group 1(2). The red spectrum is the breyite holotype from Brenker *et al*. (2021) in both **(a)** and **(b)**, whereas our data are plotted in black.

Supplementary Information References

Adams, H.G., Cohen, L.H., Rosenfeld, J.L. (1975) Solid inclusion piezothermometry I: Comparison dilatometry. *American Mineralogist* 60, 574–583. https://pubs.geoscienceworld.org/msa/ammin/article-abstract/60/9-10/944/543164/Solid-inclusion-piezothermometry-I-Comparison?redirectedFrom=fulltext

Angel, R.J., Alvaro, M., Nestola, F., Mazzucchelli, M.L. (2015) Diamond thermoelastic properties and implications for determining the pressure of formation of diamond–inclusion systems. *Russian Geology and Geophysics* 56, 211–220. https://doi.org/10.1016/j.rgg.2015.01.014

Angel, R.J., Alvaro, M., Nestola, F. (2022) Crystallographic Methods for Non-destructive Characterization of Mineral Inclusions in Diamonds. *Reviews in Mineralogy and Geochemistry* 88, 257–305. https://doi.org/10.2138/rmg.2022.88.05

Anzolini, C., Angel, R.J., Merlini, M., Derzsi, M., Tokár, K., Milani, S., Krebs, M.Y., Brenker, F.E., Nestola, F., Harris, J.W. (2016) Depth of formation of $CaSiO_3$-walstromite included in super-deep diamonds. *Lithos* 265, 138–147. https://doi.org/10.1016/j.lithos.2016.09.025

Brenker, F.E., Nestola, F., Brenker, L., Peruzzo, L., Harris, J.W. (2021) Origin, properties, and structure of breyite: The second most abundant mineral inclusion in super-deep diamonds. *American Mineralogist* 106, 38–43. https://doi.org/10.2138/am-2020-7513

Lafuente, B., Downs, R.T., Yang, H., Stone, N. (2016) 1. The power of databases: the RRUFF project. In: Armbruster, T., Danisi, R.M. (Eds.) *Highlights in Mineralogical Crystallography*. De Gruyter, Berlin, 1–30. https://doi.org/10.1515/9783110417104-003

Rosenfeld, J.L., Chase, A.B. (1961) Pressure and temperature of crystallization from elastic effects around solid inclusion minerals? *American Journal of Science* 259, 519–541. https://doi.org/10.2475/ajs.259.7.519

Wojdyr, M. (2010) *Fityk*: a general-purpose peak fitting program. *Journal of Applied Crystallography* 43, 1126–1128. https://doi.org/10.1107/S0021889810030499